Twisting of the Second Transmembrane α-Helix of the Mitochondrial ADP/ATP Carrier during the Transition between Two Carrier Conformational States†

Yoshitaka Kihira,[‡,§] Akihiro Iwahashi,[‡,§] Eiji Majima,[||] Hiroshi Terada,[⊥] and Yasuo Shinohara*[,‡,§,@]

Faculty of Pharmaceutical Sciences, University of Tokushima, Shomachi-1, Tokushima 770-8505, Japan, Institute for Genome Research, University of Tokushima, Kuramotocho-3, Tokushima 770-8503, Japan, APRO Life Science Institute, Inc., Muyacho, Naruto 772-0001, Japan, Faculty of Pharmaceutical Sciences, Tokyo University of Science, Yamazaki 2641, Noda 278-8510, Japan, and Single-Molecule Bioanalysis Laboratory, National Institute of Advanced Industrial Science and Technology (AIST), Hayashicho 2217-14, Takamatsu 761-0395, Japan

Received March 25, 2004; Revised Manuscript Received September 18, 2004

ABSTRACT: To investigate the structural and functional features of the second α-helical transmembrane segment (TM2) of the mitochondrial ADP/ATP carrier (AAC), we adopted cysteine scanning mutagenesis analysis. Single-cysteine mutations of yeast AAC were systematically introduced at residues 98−106 in TM2, and the mutants were treated with the fluorescent SH reagent eosin-5-maleimide (EMA). EMA modified different amino acid residues of α-helical TM2 between the two distinct carrier conformations, called the m-state and the c-state, in which the substrate recognition site faces the matrix and cytosol, respectively. When amino acids in the helix were projected on a wheel plot, these EMA-modified amino acids were observed at distinct sides of the wheel. Since the SH reagent specifically modified cysteine in the water-accessible environment, these results indicate that distinct helical surfaces of TM2 faced the water-accessible space between the two conformations, possibly as a result of twisting of this helix. In the recently reported crystal structure of bovine AAC, several amino acids faced cocrystallized carboxyatractyloside (CATR), a specific inhibitor of the carrier. These residues correspond to those modified with EMA in the yeast carrier in the c-state. Since the binding site of CATR is known to overlap that of the transport substrate, the water-accessible space was thought to be a substrate transport pathway, and hence, the observed twisting of TM2 between the m-state and the c-state may be involved in the process of substrate translocation. On the basis of the results, the roles of TM2 in the transport function of AAC were discussed.

The ADP/ATP carrier (AAC)[1] in the mitochondrial inner membrane, a carrier belonging to the mitochondrial solute carrier family, mediates the export of ATP into the cytosol with the import of ADP into the mitochondrial matrix in the terminal step of oxidative phosphorylation (*1*, *2*). The carrier has two distinct conformations named the c-state and m-state, in which the substrate recognition site of the carrier faces the cytosolic side and matrix side, respectively. AAC catalyzes the exchange of substrates ADP and ATP by interconversion between the two states and is considered to be dimeric when functioning (*3*−*6*). Two types of specific AAC inhibitors have been identified; one fixes the carrier in the c-state and the other the carrier in the m-state. Atractyloside (ATR) and carboxyatractyloside (CATR) are examples of the first type of inhibitor. They are membrane impermeable and interact with AAC from the cytosolic side and fix the carrier in the c-state. The second type is bongkrekic acid (BKA), which is membrane permeable and accesses the carrier from the matrix side and fixes it in the m-state (*1*, *2*, *7*).

AAC is constructed from approximately 300 amino acid residues, and the sequence has a tripartite structure consisting of three homologous repeats, each with ∼100 amino acid residues (*1*, *2*, *7*). Each repeat has two transmembrane (TM) α-helices connected by large hydrophilic loops in the matrix (LM1−3), and the repeats are linked by shorter loops in the cytosol (LC1 and -2; Figure 1). The structural and functional features of AAC have been investigated by the use of bovine type 1 AAC (bAAC1) and yeast type 2 AAC (yAAC2), the sequences of which are ∼50% identical. Studies on the reactivity of SH reagents with the LMs of bAAC1, each of which has one cysteine residue, showed that they change their structure between the c-state and the m-state (*8*−*11*). Especially LM1 drastically changes its conformation and functions as a gate to open and shut the substrate transport

† This work was supported by a grant-in-aid for scientific research from the Ministry of Education, Science, and Culture of Japan (Grant 14370746 to Y.S.).

* To whom correspondence should be addressed: Institute for Genome Research, University of Tokushima, Kuramotocho-3, Tokushima 770-8503, Japan. Fax: +81-88-633-9146. E-mail: yshinoha@genome.tokushima-u.ac.jp.

‡ Faculty of Pharmaceutical Sciences, University of Tokushima.

§ Institute for Genome Research, University of Tokushima.

|| APRO Life Science Institute, Inc.

⊥ Tokyo University of Science.

@ National Institute of Advanced Industrial Science and Technology.

[1] Abbreviations: AAC, ADP/ATP carrier; yAAC2, yeast type 2 AAC; bAAC1, bovine type 1 AAC; ATR, atractyloside; CATR, carboxyatractyloside; BKA, bongkrekic acid; EMA, eosin-5-maleimide; PAGE, polyacrylamide gel electrophoresis; DTT, dithiothreitol; SDS, sodium dodecyl sulfate; TM, transmembrane region; LM1, first matrix loop.

10.1021/bi0494222 CCC: $27.50 © 2004 American Chemical Society
Published on Web 11/10/2004

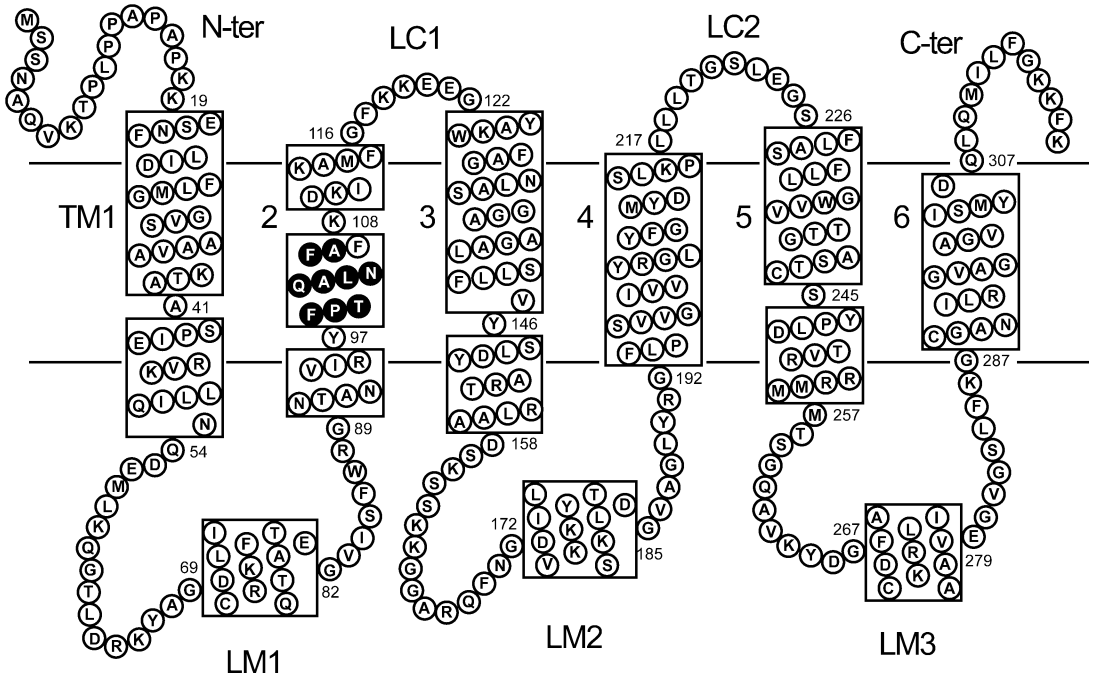

FIGURE 1: Topology of yAAC2. This model of six transmembrane α-helical spans was developed from the results of a previous study (*18*). The sequence of yAAC2 is shown using the one-letter amino acid code. The rectangular boxes represent α-helices. The black circles highlight the residues of the carrier subjected to cysteine scanning mutagenesis. In the model, the first and second loops facing the cytosol are denoted LC1 and LC2, respectively, and the first, second, and third loops facing the matrix are denoted LM1−3, respectively. Transmembrane α-helices are denoted TM.

pore at the matrix side. These results suggest that the conformation of the carrier drastically changes while it transports substrates. A drastic conformational change in LM1 was also observed in yAAC2 (*12*). Each of the even-numbered transmembrane regions of both bovine and yeast carriers has an arginine residue that is functionally important (*1*, *13*, *14*). Furthermore, chemical modification studies using the lysine reagent pyridoxal 5-phosphate and fluorescence measurement studies also indicated that the conformation of AAC changes between the two distinct AAC states (*15*−*17*). Therefore, the conformational change in the whole AAC molecule is tightly associated with its substrate transport function. The crystal structure of bAAC1 fixed in the c-state by CATR was recently reported (*18*). Its crystal structure provided us much information to help us understand better the transport mechanism of AAC and of other mitochondrial solute carriers. However, further detailed studies on the structures associated with transport function seem to be required for a better understanding its transport mechanism.

Recently, mutagenesis and chemical modification studies on mitochondrial carriers of citrate and oxoglutarate were actively carried out (*19*−*21*). In this study, we investigated the structural change in yeast AAC between its two carrier states by using cysteine scanning mutagenesis and chemical modification. On the basis of our results, we also discussed the transport mechanism of AAC.

EXPERIMENTAL PROCEDURES

Materials. The haploid strain of *Saccharomyces cerevisiae* W303-1B (MATα *ade2-1 leu2-3,112 his3-22,15 trp1-1 ura3-1 can1-100*) (*22*) was obtained from Dr. Shimizu (Osaka University, Osaka, Japan). The AAC-disrupted strain of WB-12 (MATα *ade2-1 leu2-3,112 his3-22,15 trp1-1 ura3-1 can1-100 aac1::LEU2 aac2::HIS3*) and the yeast shuttle vector pRS314-YA2P were prepared as described previously (*23*). [^{14}C]ADP was obtained from DuPont-New England Nuclear (Wilmington, DE), CATR from Sigma (St. Louis, MO), and EMA from Molecular probes (Eugene, OR). Other materials and reagents were of the highest grade commercially available.

Mutagenesis of AAC and Culture Condition of Yeast Cells. Mutant transporters were generated by site-directed mutagenesis of the Cys-less yAAC2, in which all four cysteines had been replaced with alanine (*12*). All mutations were confirmed by DNA sequencing. The DNA fragments that were made were subcloned into pRS314-YA2P for transformation of the AAC-disrupted yeast strain, as described previously (*23*). Yeast cells were grown at 30 °C in YP medium consisting of 1% yeast extract and 2% bactopeptone supplemented with either 2% glucose (YPD), 2% galactose (YPGal), or 3% glycerol (YPGly) as a carbon source. For selection of transformants, the cells were grown at 30 °C in SD medium consisting of 0.67% yeast nitrogen base without amino acids and 2% glucose supplemented with standard concentrations of nutritional requirements when necessary (*24*). Solid media contained 2% Bacto-Agar (Difco Laboratories) (*23*).

Detection of AAC. Yeast mitochondria were isolated as described previously (*23*). For detection of AAC in mitochondria, mitochondrial protein was subjected to SDS−PAGE and Western blot analysis using antiserum against synthetic peptides of the yAAC2-specific sequence (Ser^{2}−Ser^{21}) (*23*).

EMA Labeling. For EMA labeling, yeast mitochondria (8 mg of protein/mL) were first pretreated with 100 μM BKA or CATR or ATR for 30 min at pH 7.4 and 25 °C, and then the samples diluted with ST [250 mM sucrose and 10 mM Tris-HCl (pH 7.4)] to 4 mg of protein/mL were incubated

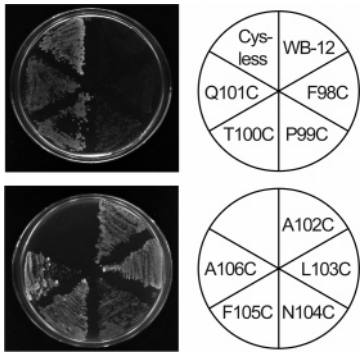

FIGURE 2: Growth of yeast cells on YPGly. The transformants were inoculated onto YPGly plates, and the growth of each was examined after 5 days at 30 °C.

with 200 μM EMA for 30 min at pH 7.4 and 0 °C in the dark. The labeling was terminated with 10 mM DTT. In the case of ATR, the period of EMA labeling was modified to 5 min. The labeled samples were subjected to SDS−PAGE on a 20% polyacrylamide gel in the dark, and the images of separated proteins were observed under UV irradiation. The degree of EMA labeling was determined by measuring the fluorescence intensities of the stained bands with an ATTO image analyzer model AE-6900 and NIH image software.

RESULTS

Construction of Single-Cysteine Mutants and Their Functional Features. Our previous study showed that cysteine residues are not essential for the transport function of the yeast type 2 ADP/ATP carrier (yAAC2), because Cys-less yAAC2, in which all four cysteine residues were substituted with alanine residues, showed ADP transport activity similar to that of wild-type yAAC2 (*12*). Thus, to investigate the structural and functional features of the second transmembrane segment (TM2) of yAAC2, in this study, we constructed a series of mutants having a unique cysteine residue at each of nine residues (98−106) in the TM2 region by use of Cys-less yAAC2 as a template. Expression vectors of these mutants were constructed, and each vector was introduced into an AAC-deficient yeast strain (WB-12), in which intrinsic genes encoding type 1 and 2 AAC had been disrupted. Transformed cells were grown on YP plates (2% Bacto-Agar plate containing 1% yeast extract and 2% bactopeptone) supplemented with glucose (YPD) or glycerol (YPGly) as the sole carbon source. AAC-disrupted strain WB-12 grew on a YPD plate (data not shown), but not on a YPGly plate, in which the nonfermentable glycerol was used as the sole carbon source (Figure 2). Cys-less yAAC2 transformants, which have the same functional features as wild-type yAAC2 (*12*), were able to grow on both plates. This result confirmed that functional AAC was expressed in mitochondria. All transformants with a single-cysteine mutant except F98C showed growth activity on both types of plates, suggesting that all mutants except F98C were functionally expressed in the mitochondrial inner membrane and that F98C had no transport activity. However, P99C, Q101C, and N104C grew slower than the parental Cys-less mutant, indicating lower transport activity of these three mutants.

Next, we examined the expression level of each mutant AAC. Isolated mitochondria expressing mutant AACs were

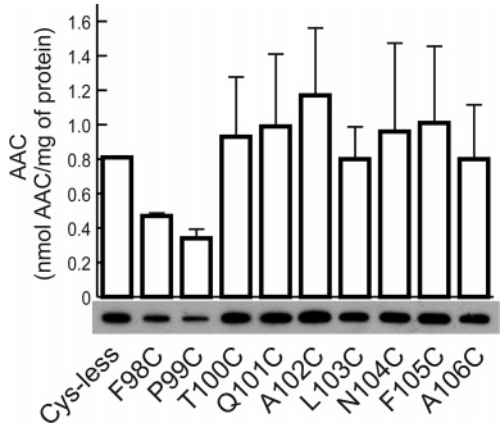

FIGURE 3: Expression levels of single-cysteine mutants in mitochondria. Mitochondria isolated from *S. cerevisiae* expressing each mutant were analyzed by Western blotting using antibodies raised against a yAAC2-specific sequence (Ser^2−Ser^{21}). Mean values ± the standard deviation ($n = 3$) of the amount of AAC protein in mitochondria are shown. The expression level of Cys-less yAAC2, reported in a previous study (*12*), is also shown as a standard.

subjected to SDS−PAGE and Western blot analysis using an antiserum against a synthetic peptide of a yAAC2-specific sequence (Ser^2−Ser^{21}). As shown in Figure 3, an expression level equal to or greater than that of the parental Cys-less mutant was observed in all mutants except F98C and P99C. Expression levels of F98C and P99C were ~50% of the parental level. However, these levels of expression were adequate for chemical modification analysis.

Chemical Modification of a Series of Single-Cysteine Mutants with EMA. We next examined the effect of the membrane impermeable fluorescent SH reagent eosin-5-maleimide (EMA) on the single-cysteine mutants of TM2. Because SH reagents selectively modify water-accessible cysteine residues (*19*, *25*−*27*), EMA also specifically modifies residues facing a water-filled surface or a substrate transport pathway. AAC interconverts between the c-state and the m-state during the transporting of substrates, and it is well-known that inhibitors CATR and BKA fix AAC in the c-state and m-state, respectively (*1*, *2*, *7*). So we conducted an EMA labeling study under conditions where conformations of AAC were fixed by CATR or BKA. Isolated mitochondria expressing each mutant were first pretreated with 100 μM CATR or BKA to fix the AAC conformation in the c-state or the m-state, respectively. Then, the samples were treated with 200 μM EMA for 30 min at pH 7.4 and 0 °C in the dark. The results are shown in Figure 4. EMA modified the 34 kDa AAC and 32.5 kDa phosphate carrier (PiC), as shown previously (*12*). Cys-less yAAC2 was not modified by EMA, indicating that EMA specifically modifies cysteine residues. In the c-state carrier fixed by CATR, it was expected that T100C, Q101C, N104C, and F105C would be modified by EMA, because the corresponding residues in the crystal structure of the bovine carrier, T83, Q84, N87, and F88, respectively, face the water-accessible surface (*18*). However, although F105C was clearly modified by EMA, no fluorescence of EMA was detected in the other mutants. Since amino acid residues T83, Q84, and N87 in bAAC1, corresponding to T100, Q101, and N104 in yAAC2, respectively, are located close to CATR in the crystal structure of bAAC1 in the presence of CATR (Figure 5) (*18*), these residues in yAAC2 would also be

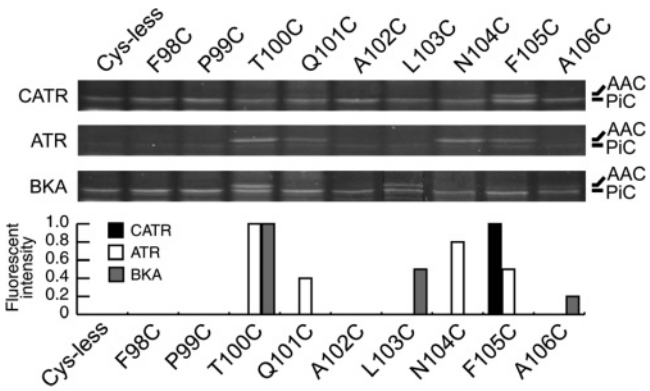

FIGURE 4: EMA labeling of single-cysteine mutants. Mitochondria of each mutant were pretreated with 100 μM BKA, CATR, or ATR for 30 min at 25 °C and then incubated with 200 μM EMA for 30 min (samples pretreated with BKA or CATR) or 5 min (samples pretreated with ATR) at pH 7.4 and 0 °C in the dark. The samples were then subjected to SDS−PAGE on 20% polyacrylamide gels in the dark. After electrophoresis, labeled AAC was visualized by irradiation with ultraviolet light. Positions of AAC and Pi carrier (PiC) are denoted. The graph shown under the photos of SDS−PAGE gels indicates the fluorescence intensity exhibited by each single-cysteine mutant of yAAC2. The degree of EMA labeling was determined by measuring the fluorescence intensities of the stained bands with an ATTO model AE-6900 image analyzer and NIH image software. The normalized fluorescence intensities relative to the highest intensity in each experiment are given.

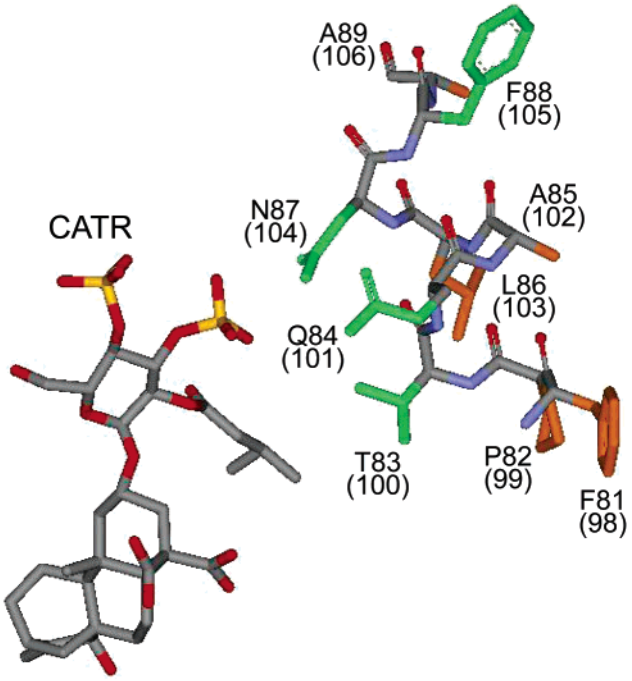

FIGURE 5: Structure of TM2 and CATR in the crystal structure of bAAC1 in the presence of CATR. The structure of amino acid residues 81−89 and the CATR molecule in the crystal structure of bAAC1 (*18*) are shown. The figure file was downloaded from a protein data bank (http://pdb.protein.osaka-u.ac.jp/pdb/) and depicted with Viewer Lite 50. Corresponding amino acid numbers of the yeast carrier are given in parentheses. Residues colored green and orange exhibit fluorescence and no fluorescence of EMA, respectively, in the ATR-bound carrier (see Figure 4).

expected to be masked by CATR when yAAC2 is treated with it. Next, we carried out an EMA labeling study by using ATR in place of CATR. ATR is a homologue of CATR, and both inhibitors fix AAC in the c-state. The dissociation

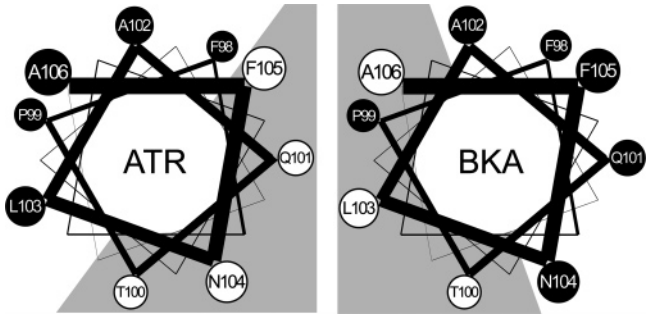

FIGURE 6: Summarized reactivities of amino acids in TM2 labeled with EMA. A helical wheel depiction of residues 98−106 in TM2 is shown. Residues labeled with white lettering on a black background and black lettering on a white background exhibit no fluorescence and fluorescence of EMA, respectively. Shaded areas represent putative water-filled spaces.

constant for ATR is approximately 10 times higher than that for CATR. Binding of ATR is, therefore, reversible, whereas that of CATR is nearly irreversible (*25*). Isolated mitochondria with each mutant were pretreated with ATR and then with 200 μM EMA under the same conditions that were used for CATR, i.e., for 30 min at pH 7.4 and 0 °C. Almost all amino acids were labeled with EMA under this condition (data not shown). The phenomenon was probably caused by a conformational change between the c-state and the m-state as a result of the release of ATR from the AAC. However, strong fluorescence was specifically observed in T100C and N104C and faint fluorescence in Q101C and F105C when the treatment time of EMA with ATR-binding mutants was shortened to 5 min (Figure 4). This specific modification of these four residues observed after the shorter treatment with EMA probably reflects the c-state carrier, because a different fluorescent pattern was observed for BKA-binding mutants (Figure 4) and bovine T83, Q84, N87, and F88 (equivalent to yeast T100, Q101, N104, and F105, respectively) face the substrate transport pore in the crystal structure (Figure 5). However, there is a possibility that the pattern of fluorescence of EMA may reflect the intermediary state between the c-state and the m-state given by the release of ATR from the AAC. This result shows that T100, Q101, N104, and F105 face the water-accessible substrate transport pore in the carrier treated with ATR. In contrast to the case for the carrier with CATR or ATR, in the m-state AAC stabilized by BKA, T100C, L103C, and A106C exhibited fluorescence of EMA (30 min treatment). Therefore, T100, L103, and A106 face the water-filled surface in the m-state, which is different from the case of the c-state carrier. The lower fluorescence observed in L103C and A106C may have been due to masking of these residues by the BKA molecule.

Because TM2 exists as an α-helix in the mitochondrial inner membrane in the c-state carrier (*18*), an α-helical wheel of residues 98−106 was prepared, as depicted in Figure 6. In the wheel, residues, T100, Q101, N104, and F105, corresponding to T83, Q84, N87, and F88 in bAAC1, respectively, facing the water-filled surface in the crystal structure of the c-state bovine carrier (Figure 5) (*18*) were concentrated on one side. On the contrary, residues 100, 103, and 106 were labeled with EMA in m-state AAC, indicating that the side having residues T100, L103, and A106 faces the transport path in this state. These results clearly indicate that different surfaces of TM2 face the substrate transport pathway between the m- and c-states, possibly as a result of

twisting of TM2 (Figure 6). P99 is in the predicted water-accessible surface in the m-state, but P99C was not modified by EMA in the m-state, perhaps due to complete masking by the BKA molecule.

DISCUSSION

The ADP/ATP carrier (AAC) has six transmembrane-spanning regions and cytosolic N- and C-termini (Figure 1). Each of the even-numbered transmembrane regions has an arginine residue that is functionally important (*1*, *13*, *14*). In addition, the AAC-specific inhibitor carboxyatractyloside (CATR) interacts with residues in the transmembrane segments, including the arginine residues (*18*). Therefore, these transmembrane segments seem to be important for the function of the AAC.

When AAC transports ADP/ATP, the conformation of AAC changes between the c-state and the m-state. In this event, loops of AAC play an important role. LM1, especially, changes its structure and works as a gate to open and close the substrate transport pore at the matrix side (*8*−*11*). LC1 also changes its conformation and serves as a gate at the cytosolic side (Y. Kihira et al., manuscript in preparation). The second transmembrane segment (TM2) positioned between LM1 and LC1 is predicted to be a structurally and functionally important segment. So we focused on TM2, in which the amino acid sequence is highly conserved among all the AACs that have been examined (*2*). The structural and functional features of TM2 were investigated by using site-directed mutagenesis and chemical modification.

For this purpose, we systematically constructed nine single-cysteine mutants, into each of which was introduced only one cysteine residue, at residues 98−106 in the central region of TM2 by using as a template Cys-less AAC (*12*), which has function comparable to that of wild-type yAAC2 (Figure 1). All transformants with each mutant except F98C grew on the glycerol medium (Figure 2), indicating that all mutants except F98C function in the mitochondria. Furthermore, the growth of transformants with P99C, Q101C, and N104C was slower than that of the parental Cys-less transformant. The expression levels of F98C and P99C proteins in mitochondria were ∼50% of the level found for the Cys-less AAC. Therefore, the reasons for no. or little growth of transformants with F98C or P99C, respectively, can, at least in part, be attributed to the inefficient expression of functional proteins in the inner mitochondrial membrane. Q101 and N104 are important residues for the transport function of AAC, because the transformants with the mutation at these positions grew slowly. In fact, Q84 and N87 in bAAC1, corresponding to Q101C and N104 in yAAC2, respectively, face the CATR molecule in the crystal structure of bAAC1 (Figure 5), and N87 is one of the residues that interact with CATR (*18*). These data suggest that the recognition site of CATR probably overlaps the site of substrate recognition.

Recently, structural and functional features of mitochondrial solute carriers were actively studied by using cysteine scanning mutagenesis and subsequent chemical modification (*19*−*21*), and the α-helical properties of transmembrane segments of some carriers were revealed. Also in this study, properties of binding of EMA to single-cysteine mutants in TM2 were investigated, and the α-helical properties of TM2 were clarified. As shown in the crystal structure of bovine AAC, residues T83, Q84, N87, and F88 face a water-filled surface, and the corresponding residues in c-state yAAC2 (T100, Q101, N104, and F105, respectively) probably face a water-filled surface as well, although EMA labeled only F105C because of the masking effect of CATR on T100, Q101, and N104. The EMA labeling study of AAC with ATR also showed that these four residues faced a water-filled surface in the c-state. However, this result may reflect an intermediary state of AAC between the c- and m-states, because ATR is released from AAC by treatment with EMA. Whether the conformational state is the c-state or an intermediary state between the c- and m-states, the residues facing the water-filled surface are T100, Q101, N104, and F105 in AAC treated with CATR or ATR. These results clearly differ from the result obtained in the m-state. Since these amino acids were located at different helical surfaces of the TM2 helix, α-helical TM2 would seem to twist itself in the transition between the two carrier conformations. Evidence of such rotation of an α-helix was also obtained in a study of the crystal structures of a calcium pump in its two distinct conformations (*26*). Rearrangement of the α-helix in this calcium pump was suggested to be involved in the change in the affinity of the pump for calcium ions, because residues interacting with the calcium ion moved away from the calcium-binding site when the conformation of the pump changed. Moreover, in the acetylcholine receptor, twisting of membrane-spanning α-helices was shown to be involved in channel opening (*27*). In the case of AAC, rotation of the second transmembrane α-helix may also be involved in the changes in its affinity for substrates and in the facilitation of substrate transport. Namely, in c-state AAC, polar residues, including N104, which may be involved in substrate recognition as discussed above, face the water-filled surface, in agreement with a feature of the crystal structure of AAC (*18*). Thus, the substrate from the cytosol is easily able to access its binding site, including N104, because of exposure of the hydrophilic surface to the substrate transport path. In contrast, in the m-state, hydrophobic residues without N104 face the surface (Figure 6), and this hydrophobic wall functions as an obstruction for the substrate from the cytosol.

As shown in our previous reports, the first matrix loop (LM1) of AAC drastically changes its structure as a gate of the transport pore between the two carrier states. In the c-state, LM1 is located close to the membrane, blocking the transport pathway to the matrix, whereas in the m-state, it is exposed to the matrix, thus opening the pathway (*8*−*11*). During our study, we also examined the structural and functional features of the first loop facing the cytosol (LC1) by chemical modification. The result showed that LC1 changes its conformation between the m- and c-state (Y. Kihira et al., manuscript in preparation). Although the recently reported crystal structure of AAC has provided deep insight into its structural features, studies on the dynamic properties of AAC are necessary for us to understand the molecular mechanism of its transport function. The adoption of a cysteine scanning approach for studying the structural and functional properties of AAC has been very useful for clarifying the transport mechanism of AAC. The results presented here have provided new insights into the dynamic structural change that occurs in AAC; however, the focus

of this study was limited to TM2 only. For a complete understanding of the transport mechanism of AAC, further studies on all regions of this carrier are required.

REFERENCES

1. Klingenberg, M. (1993) Dialectics in carrier research: the ADP/ATP carrier and the uncoupling protein, *J. Bioenerg. Biomembr. 25*, 447−457.
2. Brandolin, G., Le Saux, A., Trezeguet, V., Lauquin, G. J., and Vignais, P. V. (1993) Chemical, immunological, enzymatic, and genetic approaches to studying the arrangement of the peptide chain of the ADP/ATP carrier in the mitochondrial membrane, *J. Bioenerg. Biomembr. 25*, 459−472.
3. Hackenberg, H., and Klingenberg, M. (1980) Molecular weight and hydrodynamic parameters of the adenosine 5′-diphosphate/adenosine 5′-triphosphate carrier in Triton X-100, *Biochemistry 19*, 548−555.
4. Block, M. R., Zaccai, G., Lauquin, G. J., and Vignais, P. V. (1982) Small angle neutron scattering of the mitochondrial ADP/ATP carrier protein in detergent, *Biochem. Biophys. Res. Commun. 109*, 471−477.
5. Huang, S. G., Odoy, S., and Klingenberg, M. (2001) Chimers of two fused ADP/ATP carrier monomers indicate a single channel for ADP/ATP transport, *Arch. Biochem. Biophys. 394*, 67−75.
6. Hatanaka, T., Hashimoto, M., Majima, E., Shinohara, Y., and Terada, H. (1999) Functional expression of the tandem-repeated homodimer of the mitochondrial ADP/ATP carrier in *Saccharomyces cerevisiae*, *Biochem. Biophys. Res. Commun. 262*, 726−730.
7. Walker, J. E. (1992) The mitochondrial transporter family, *Curr. Opin. Struct. Biol. 2*, 519−526.
8. Majima, E., Shinohara, Y., Yamaguchi, N., Hong, Y.-M., and Terada, H. (1994) Importance of loops of mitochondrial ADP/ATP carrier for its transport activity deduced from reactivities of its cysteine residues with the sulfhydryl reagent eosin-5-maleimide, *Biochemistry 33*, 9530−9536.
9. Majima, E., Ikawa, K., Takeda, M., Hashimoto, M., Shinohara, Y., and Terada, H. (1995) Translocation of loops regulates transport activity of mitochondrial ADP/ATP carrier deduced from formation of a specific intermolecular disulfide bridge catalyzed by copper-o-phenanthroline, *J. Biol. Chem. 270*, 29548−29554.
10. Terada, H., and Majima, E. (1997) Important role of loops in the transport activity of the mitochondrial ADP/ATP carrier, *Prog. Colloid Polym. Sci. 106*, 192−197.
11. Hashimoto, M., Majima, E., Goto, S., Shinohara, Y., and Terada, H. (1999) Fluctuation of the first loop facing the matrix of the mitochondrial ADP/ATP carrier deduced from intermolecular cross-linking of Cys56 residues by bifunctional dimaleimides, *Biochemistry 38*, 1050−1056.
12. Hatanaka, T., Kihira, Y., Shinohara, Y., Majima, E., and Terada, H. (2001) Characterization of loops of the yeast mitochondrial ADP/ATP carrier facing the cytosol by site-directed mutagenesis, *Biochem. Biophys. Res. Commun. 286*, 936−942.
13. Nelson, D. R., Lawson, J. E., Klingenberg, M., and Douglas, M. G. (1993) Site-directed mutagenesis of the yeast mitochondrial ADP/ATP translocator. Six arginines and one lysine are essential, *J. Mol. Biol. 230*, 1159−1170.
14. Klingenberg, M., and Nelson, D. R. (1994) Structure−function relationships of the ADP/ATP carrier, *Biochim. Biophys. Acta 1187*, 241−244.
15. Bogner, W., Aquila, H., and Klingenberg, M. (1986) The transmembrane arrangement of the ADP/ATP carrier as elucidated by the lysine reagent pyridoxal 5-phosphate, *Eur. J. Biochem. 161*, 611−620.
16. Brandolin, G., Dupont, Y., and Vignais, P. V. (1985) Substrate-induced modifications of the intrinsic fluorescence of the isolated adenine nucleotide carrier protein: Demonstration of distinct conformational states, *Biochemistry 24*, 1991−1997.
17. Le Saux, A., Roux, P., Trezeguet, V., Fiore, C., Schwimmer, C., Dianoux, A.-C., Vignais, P. V., Brandolin, G., and Lauquin, G. J.-M. (1996) Conformational change of the yeast mitochondrial adenosine diphosphate/adenosine triphosphate carrier studied through its intrinsic fluorescence. 1. Tryptophanyl residues of the carrier can be mutated without impairing protein activity, *Biochemistry 35*, 16116−16124.
18. Pebay-Peyroula, E., Dahout-Gonzalez, C., Kahn, R., Trezeguet, V., Lauquin, G. J., and Brandolin, G. (2003) Structure of mitochondrial ADP/ATP carrier in complex with carboxyatractyloside, *Nature 426*, 39−44.
19. Kaplan, R. S., Mayor, J. A., Brauer, D., Kotaria, R., Walters, D. E., and Dean, A. M. (2000) The yeast mitochondrial citrate transport protein. Probing the secondary structure of transmembrane domain IV and identification of residues that likely comprise a portion of the citrate translocation pathway, *J. Biol. Chem. 275*, 12009−12016.
20. Stipani, V., Cappello, A. R., Daddabbo, L., Natuzzi, D., Miniero, D. M., Stipani, I., and Palmieri, F. (2001) The mitochondrial oxoglutarate carrier: cysteine-scanning mutagenesis of transmembrane domain IV and sensitivity of Cys mutants to sulfhydryl reagents, *Biochemistry 40*, 15805−15810.
21. Morozzo della Rocca, B., Lauria, G., Venerini, F., Palmieri, L., Polizio, F., Capobianco, L., Stipani, V., Pedersen, J., Cappello, A. R., Desideri, A., and Palmieri, F. (2003) The mitochondrial oxoglutarate carrier: structural and dynamic properties of transmembrane segment IV studied by site-directed spin labeling, *Biochemistry 42*, 5493−5499.
22. Lawson, J. E., and Douglas, M. G. (1988) Separate genes encode functionally equivalent ADP/ATP carrier proteins in *Saccharomyces cerevisiae*. Isolation and analysis of AAC2, *J. Biol. Chem. 263*, 14812−14818.
23. Hashimoto, M., Shinohara, Y., Majima, E., Hatanaka, T., Yamazaki, N., and Terada, H. (1999) Expression of the bovine heart mitochondrial ADP/ATP carrier in yeast mitochondria: Significantly enhanced expression by replacement of the N-terminal region of the bovine carrier by the corresponding regions of the yeast carrier, *Biochim. Biophys. Acta 1409*, 113−124.
24. Treco, D. A., and Lundblad, V. (1993) *Saccharomyces cerevisiae*, in *Current Protocols in Molecular Biology* (Ausubel, F. M., et al., Eds.) Chapter 13.1, John Wiley, New York.
25. Klingenberg, M. (1974) The mechanism of the mitochondrial ADP, ATP carrier as studied by the kinetics of ligand binding, in *Dynamics of Energy-Transducing Membranes* (Ernster, L., Estabrook, R. W., and Slater, E. C., Eds.) pp 511−528, Elsevier, Amsterdam.
26. Toyoshima, C., and Nomura, H. (2002) Structural changes in the calcium pump accompanying the dissociation of calcium, *Nature 418*, 605−611.
27. Miyazawa, A., Fujiyoshi, Y., and Unwin, N. (2003) Structure and gating mechanism of the acetylcholine receptor pore, *Nature 423*, 949−955.

BI0494222